Concepts and Design of Novel Integrated Photonic Devices based on Silicon-organic Hybrid Technology

Patrick Steglich[1,2], Mauro Casalboni[2] and Sigurd Schrader[1]

[1]*Faculty of Engineering and Natural Sciences, University of Applied Sciences Wildau, Wildau, Germany*
[2]*Department of Industrial Engineering, University of Rome "Tor Vergata", Rome, Italy*

1 RESEARCH PROBLEM

This doctoral thesis is about the development of integrated photonic devices through the implementation of electro-optical organic materials in a CMOS-like production line. Slot-waveguide structures are the key element in order to integrate organic materials into silicon photonics. For that reason, slot-waveguides have been employed in order to develop high-speed modulators for telecommunication interconnects (Weimann et al., 2014).

The major advantage of slot-waveguides is the fact that the guided light is confined in between two silicon rails (Almeida et al., 2004). For that reason the light is forced to interact directly with the surrounding material. Figure 1 shows a detailed cross-sectional
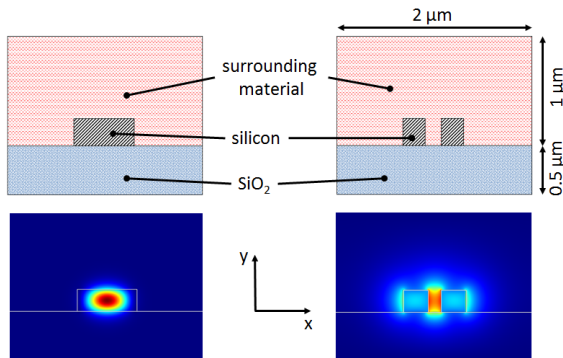

Figure 1: Cross-sectional view of a SOI strip-waveguide (left) and a SOI slot-waveguide (right). The pictures below show the optical field amplitude distribution. Both waveguide structures are on top of a buried oxide (BOX) substrate. The slot-waveguide structure shows enhanced field intensity in the slot interior.

view and compares the guided optical field in a strip-waveguide to a slot-waveguide.

The reason for this high confinement in-between the silicon rails is the large-index contrast of the high-index silicon and the low-index surrounding material. At the interface the normal electric field, which is according to Figure 1 the E_x field, undergoes a large dis-

continuity. This results in a field enhancement in the low-index region which is proportional to the ratio of the dielectric constant of the surrounding material to that of silicon.

The high confinement inside the slot is of special benefit for electro-optical applications. The so called silicon-organic hybrid (SOH) technology uses organic materials with exceptional high linear electro-optical coefficients as surrounding material (Leuthold et al., 2013). Current electro-optic modulators are based on semiconductors like silicon. In silicon photonics, fundamental speed limitations are related to carrier injection and removal (Vivien and Pavesi, 2013). Therefore, parametric processes are impaired by nonparametric processes like two-photon absorption and become to the main speed limiting factor. Additionally, silicon has a lack of linear electro-optical coefficients. All this can be overcome by using organic materials with nonlinear optical properties as active material.

The most challenging issue of SOH technology based slot-waveguides is the compatibility with common complementary-metal-oxide-semiconductor (CMOS) fabrication processes since such integrated photonic devices need a high integration rate and a cost efficient mass production environment.

For that reason, one focus of this thesis lies on design trade-offs and on the development of an approach in order to improve silicon-on-insulator (SOI) slot-waveguide structures for a CMOS-like production environment.

Beside the theoretical investigations there are several critical issues during the fabrication process. The slot width is limited due to common lithography restrictions and has a high side-wall roughness after etching which leads to optical losses. After the Back-End-Of-Line (BEOL) which includes the metal contacts, as it can be seen in Figure 2, it is necessary to open the slot-waveguide structures in order to deposit the organic material inside the slot interior. This step is critical because a combination of dry and wet etching is necessary. Nevertheless, it is necessary in order to maintain CMOS compatibility before the deposi-

striploaded slot-waveguide

organic material cladding

BOX

metal electrode

silicide

BOX

n doped silicon stripload
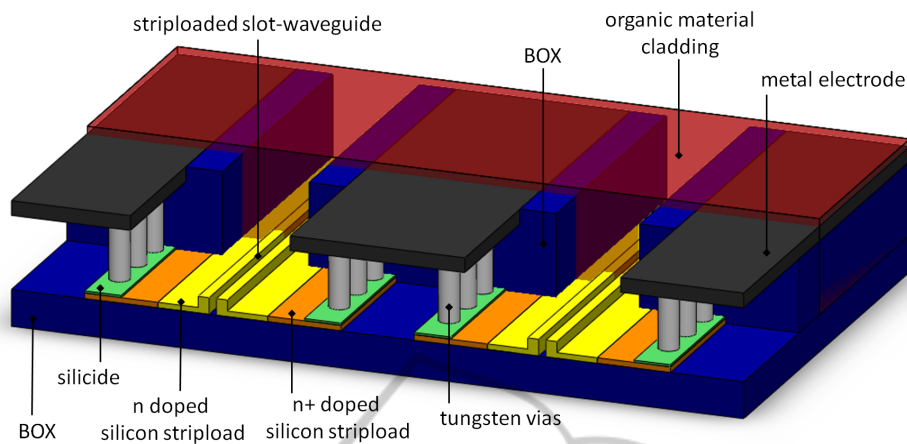
n+ doped silicon stripload

tungsten vias

Figure 2: Cross section of two full implemented slot-waveguides with stripload and electrode connection (not to scale). The slot-waveguide structure has to be opened in order to fill-out the slot with a nonlinear optical cladding. The slot-waveguide rails are connected by tungsten vias to metal contacts. In this configuration, both slot-waveguides can be used as phase shifter for a Mach-Zehnder modulator.

tion of organic material.

Selection and deposition of organic materials with large linear electro-optical coefficients is another critical task. State of the art SOH modulators using a novel class of so-called monolithic electro-optic materials in order to yield high in-device electro-optic coefficients by avoiding dipole-dipole interactions (Dalton et al., 2010; Palmer et al., 2014).

2 OUTLINE OF OBJECTIVES

The main objective of the thesis is the implementation of electro-optical organic materials in a CMOS-like production environment in order to develop integrated photonic devices such as novel electro-optical modulators based on slot-waveguide structures. Consequently, the scope of this thesis is the conception, design, and modelling of passive and active photonic components like strip-to-slot mode-converter, grating coupler, slot-waveguide structures and electrical contacts. Novel design concepts such as partially slotted ring resonators and Fabry-Perot-Interferometer with slotted cavity will be developed. Besides theoretical investigations, device fabrication and evaluation as well as deposition of electro-optical organic materials are objectives of the thesis. The organic materials need to have high thermal, photochemical and long-term orientational stability as well as a minimized self-aggregation to avoid scattering losses. Furthermore, large electro-optical coefficients are necessary in order to reduce the drive voltage of the modulators. For this reason one part of the thesis is to find appropriate organic materials and deposition methods. This implies the characterisation of linear and nonlin-

ear optical properties. In order to deposit the organic materials on the slot-waveguide structure a new approach will be developed which includes an etching procedure to open the slot-waveguide structure from the backside of the SOI wafer.

3 STATE OF THE ART

The Karlsruhe Institute of Technology reported in 2013 and 2014 several silicon-organic hybrid modulators based on a Mach-Zehnder interferometer operating at 10 Gbit/s, 12.5 Gbit/s, 40 Gbit/s, 84 Gbit/s, and 112 Gbit/s (Palmer et al., 2013b; Korn et al., 2013; Leuthold et al., 2013; Palmer et al., 2014; Korn et al., 2014). They have demonstrated advanced modulation formats such as 16QAM (Quadrature Amplitude Modulation) as well as OOK (On-Off Keying), BPSK (Binary Phase Shift Keying) and 8-ASK (Amplitude Shift Keying) signals (Korn et al., 2013; Palmer et al., 2013c). This is possible due to the fact that organic materials have less free-carrier dispersion which normally leads to an intrinsic coupling of amplitude and phase.

A silicon-polymer hybrid slot waveguide ring-resonator modulator with a 6 dB bandwidth of 1 GHz, a device tunability of 12.7 pm/V, and a Q-factor of 5000 were fabricated with 193 nm optical lithography (Gould et al., 2011).

Palmer et al. published in 2013 strip-to-slot mode-converter with record-low losses of about 0.02 dB and negligible reflections between 1480 nm and 1580 nm (Palmer et al., 2013a). Yang Liu et al. developed in 2011 a so called strip to strip-loaded slot mode converter with losses around 0.81 dB (Liu et al., 2011).

The deposition of organic materials is typically done by spin-coating but vapour deposition is more suitable. Spin-coating is critical because the organic material has to fill-out the interior of the slot homogeneously. With spin-coating, it is not guaranteed that the slot will be filled due to the centrifugal force and due to the fact that the polymer system is liquid. With its viscosity and surface tension it precludes the polymer system from filling out the whole interior of the slot homogeneously. Commercially available and reliable organic materials such as $M3$ (commercialized by GigOptix Inc.) have been successfully used for several slot-waveguide based electro-optical modulators like in (Palmer et al., 2013b; Leuthold et al., 2013; Korn et al., 2013; Palmer et al., 2013c). Special methods have been developed in order to fill-out the interior of sub-micrometer slot-waveguide structures with such solid crystals (Korn et al., 2014). Furthermore, multi-chromophore dendritic molecules, guest-host and side-chain polymersystems have been used as electro-optical cladding (Palmer et al., 2014).

In the last decade integrated photonic sensors based on slot-waveguide ring-resonators have also been proposed (Dell'Olio and Passaro, 2007) and developed (Barrios et al., 2007). In case of label-free bio-sensors it has been shown that the sensitivity of slot-waveguides is more than three times higher compared to conventional silicon strip-waveguides (Claes et al., 2009).

There are several publications about field confinement factors of slot-waveguide structures. These structures consist of vertical silicon rails (Robinson et al., 2008) or multiple nanolayers (Feng et al., 2006). However, none of them consider SOI slot-waveguides with typical geometrical dimensions for CMOS-like production processes.

4 METHODOLOGY

4.1 Simulation of Slot-waveguides

For the calculation of waveguide eigenmodes we employing a commercial full-vectorial 2D finite element method (FEM) based mode solver from COMSOL Multiphysics®. Doing this we sweep several parameters like the silicon rail width and slot width whereas the height is fixed to 220 nm. Assuming a wavelength of 1550 nm, the refractive index for the silicon is $n_{si} = 3.48$ and for the BOX substrate $n_{box} = 1.444$ (Palik, 1997; Tsang et al., 2002). The refractive index of the surrounding material n_{sm} is variable because it can be air, gas, fluid or an optical nonlinear material, depending on the application. In the following

we will use n_{clad} as cladding refractive index instead of n_{sm} because our simulation will use an organic cladding material. For our simulations we consider a total domain of $D_{tot} = 3 \ \mu m^2$ which is illustrated in Figure 1.

In order to yield the mode field distribution and effective refractive index, the refractive index distribution $n(x,y)$ for the structure shown in Figure 1 need to be declared to calculate eigenvalues and eigenfunctions of the wave equation

$$\nabla \times (\nabla \times \mathbf{E}) - k_0^2 n^2 \mathbf{E} = 0, \tag{1}$$

where k_0 is the wave number in free space. By doing this we get the optical field distribution for the quasi-TE and quasi-TM mode as shown in Figure 3. In the following we will neglect the quasi-TM mode because it is over two times of magnitude smaller than the quasi-TE mode.
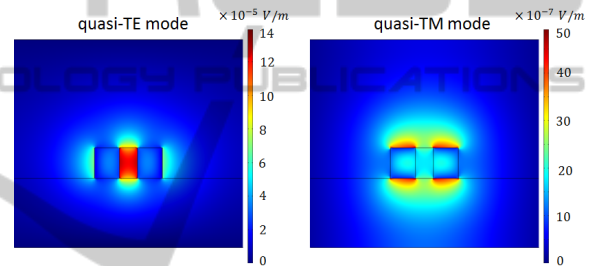

Figure 3: Optical field distribution for the quasi-TE and quasi-TM mode of a SOI slot-waveguide.

4.1.1 Field Confinement Factor of Slot-waveguides

In order to design, develop and improve slot-waveguide structures for applications in the field of biophotonic or high-speed modulators it is necessary to calculate characteristic values which describe the confinement and therefore the interaction of light with the surrounding material. One figure of merit of how well the guided modal field is confined in a certain region is the so-called field confinement factor.

The field confinement factor is usually defined as the ratio of the time averaged power flow in the domain of interest (D_{int}) to the time averaged power flow inside the total domain (D_{tot})

$$\Gamma = \frac{\int\int_{D_{int}} Re\{[\mathbf{E} \times \mathbf{H}^*] \cdot \mathbf{e}_z\} \ \mathrm{d}x\mathrm{d}y}{\int\int_{D_{tot}} Re\{[\mathbf{E} \times \mathbf{H}^*] \cdot \mathbf{e}_z\} \ \mathrm{d}x\mathrm{d}y}. \tag{2}$$

E and H are the electric and magnetic field vectors, respectively, and e_z is the unit vectors in z direction. There are three different cases in order to choose

the domain of interest. In case of common strip-waveguides the domain of interest is equal to the core region, $D_{int}=D_{core}$. In contrast to that, for bio-sensing applications the region of the cover medium is considered to be the domain of interest, $D_{int}=D_{cover}$, which is valid for strip- and slot-waveguides as well. Considering slot-waveguides for electro-optical modulators the domain of interest is equal to the slot region, $D_{int}=D_{slot}$. All possible domains of interest are illustrated in Figure 4.
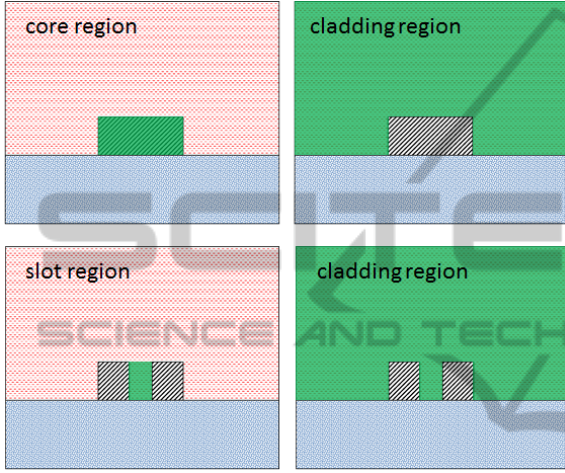

Figure 4: Domains of interest: core D_{core}, cladding D_{clad} and slot D_{slot} regions are highlighted in green.

In case of low-index-contrast waveguides, Equation 2 can be simplify using the linear relationship between the electric and magnetic fields

$$\frac{1}{2} \int \int Re\{[\mathbf{E} \times \mathbf{H}^*] \cdot \mathbf{e}_z\} \, \mathrm{d}x\mathrm{d}y = \frac{1}{2} \frac{\beta}{\omega\mu_0} \int \int |\mathbf{E}|^2 \, \mathrm{d}x\mathrm{d}y, \quad (3)$$

which leads to

$$\Gamma = \frac{\int \int_{D_{int}} |\mathbf{E}|^2 \, \mathrm{d}x\mathrm{d}y}{\int \int_{D_{tot}} |\mathbf{E}|^2 \, \mathrm{d}x\mathrm{d}y}. \quad (4)$$

However, for high-index-contrast waveguides and especially for slot-waveguides this linear relationship does not apply since they must satisfy different boundary conditions (Robinson et al., 2008). Because of that, in this work all confinement factors are calculated according to Equation 2.

4.1.2 Effective Nonlinear Area of Slot-Waveguides

A figure of merit of how well the waveguide geometry supports the nonlinear interaction is the so called effective nonlinear area (Koos et al., 2007). The smaller the effective nonlinear area provided by the waveguide structure the higher the nonlinear interaction which is important for electro-optical modulators.

For the analysis of low-index-contrast systems, it is usually assumed that the gradient of the dielectric constant is approximately zero in the entire cross section. But this approximation is not valid for high-index-contrast material systems. Therefore, Koos et al. derived the effective nonlinear area for high-index-contrast waveguides in 2007 by using the slowly varying envelope approximation (Koos et al., 2007). The effective nonlinear area results then from the nonlinear Schrödinger equation

$$A_{eff} = \frac{Z_0^2}{n_{clad}^2} \cdot \frac{\left| \int \int_{D_{tot}} Re\{[\mathbf{E} \times \mathbf{H}^*] \cdot \mathbf{e}_z\} \, \mathrm{d}x\mathrm{d}y \right|^2}{\int \int_{D_{int}} |\mathbf{E}|^4 \, \mathrm{d}x\mathrm{d}y}, \quad (5)$$

with the free-space wave impedance $Z_0 = \sqrt{\mu_0/\varepsilon_0} \approx 377 \, \Omega$. In our case is the domain of interest equal to the cladding domain, $D_{int} = D_{slot}$. In case of low-index-contrast material systems it can be assumed that $n_{core} \approx n_{clad} \approx n_{box} \approx n_{int}$, and the longitudinal field becomes negligible (Koos et al., 2007). Furthermore, the transverse components of the electrical field E and the magnetic field H can be approximated by a scalar function F with the condition $E \approx F \cdot e_x$ and $H \approx (n_{int}/Z_0)F \cdot e_y$ where e_x and e_y are the unit vectors in x and y direction, respectively (Koos et al., 2007). Further it can be stated that $D_{int} = D_{tot}$ if the nonlinearity is homogeneous in D_{tot}. Now Equation 5 becomes simplified to

$$A_{eff} = \frac{\left(\int \int_{D_{tot}} |F|^2 \, \mathrm{d}x\mathrm{d}y \right)^2}{\int \int_{D_{int}} |F|^4 \, \mathrm{d}x\mathrm{d}y}, \quad (6)$$

which is similar to the common definition of an effective area (Agrawal, 2012).

4.2 Concept Development and CMOS Implementation

An appropriate approach to implement nonlinear organic materials in silicon based fabrication environment is the use of striploaded slot-waveguides. A detailed cross sectional view of two parallel implemented slot-waveguides is depicted in Figure 2. Through a doped silicon stripload and tungsten vias, the slot-waveguides are directly connected to the metal electrodes. The tungsten vias are connected

with the silicon stripload through a thin silicide layer for better connectivity and conductivity.

A SOI slot-waveguide typically consists of two silicon rails with a fixed height of 220 nm due to common CMOS-like production restrictions. As it can be seen in Figure 1 both silicon rails are located on top of a buried oxide (BOX) substrate and are separated from each other by a slot width s and have a rail width w.

The SOH modulators will be fabricated in a 0.13 μm SiGe BiCMOS production line at the Institute of High-Performance Microelectronics (IHP) in Frankfurt(Oder), Germany. In order to transfer the new concepts into a CMOS production routine, it is necessary to develop a design with 2D layers. Each layer defines a production step such as etching or deposition at a certain area. The design will be done with the CAD software TexEDA®. Every single layer has to be defined with careful attention on the production restrictions and design rules for the fabrication process.

Figure 5 shows the concept of a SOH slot-waveguide ring resonator without silicon striploads. The ring is partially slotted in order to obtain higher Q-factors.
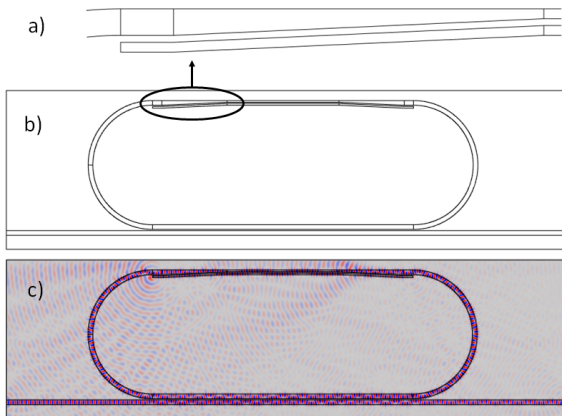

Figure 5: a) Strip-to-slot mode-converter. b) SOH slot-waveguide ring resonator. c) Optical field distribution of the SOH slot-waveguide ring resonator modulator.

5 EXPECTED OUTCOME

5.1 Theoretical Investigations

Theoretical investigations are mainly done in order to find optimized geometrical parameters for slot-waveguide structures. Figures of merit such as field confinement factors and effective nonlinear area are calculated and published (Steglich et al., 2014;

Steglich et al., 2015a; Steglich et al., 2015b). Further simulations will concentrate on design improvements of strip-to-slot mode-converter in order to decrease optical losses.

5.2 Device Fabrication

First SOH modulator concepts are transferred to an appropriate design and fabricated at the IHP in a 0.13 μm SiGe BiCMOS production line using 200 mm SOI wafers and 248 nm DUV lithography. For instance, SOH slot-waveguide ring resonator modulators with a circumferences of 69.3 μm and 95.5 μm have been fabricated. The transmission spectrum is shown in Figure 6. Measured Q-factor, Full-Width-Half-Maximum (FWHM) and Free-Spectrum-Range (FSR) of three fabricated micro slot-waveguide ring resonators are listed in Table 1. The stated slot widths are not yet confirmed by the results of a focus ion beam and may therefore slightly differ from the expected value. We expect a Q-factor of about 29000 which is almost six times higher compared to state of the art SOH slot-waveguide ring resonator modulators (Gould et al., 2011). Future work will concentrate on the deposition of organic materials from the vacuum instead of spin-coating. The advantage is the possibility to fill-out trenches with high aspect ratios at the backside of SOI wafers. This is necessary to open slot-waveguide structures without the destruction of the BEOL and in order to deposit organic materials without covering the metal electrodes.
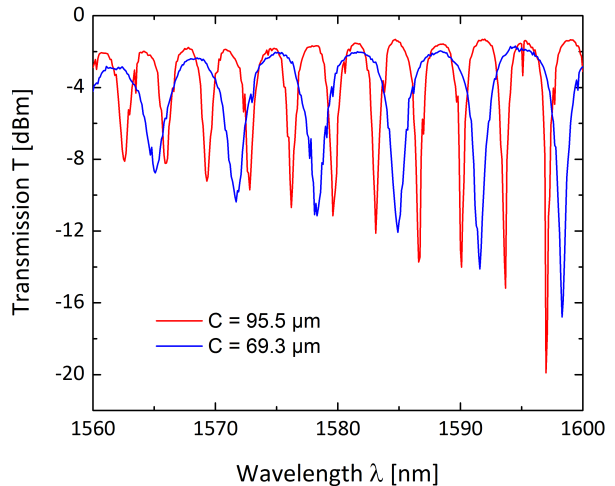

Figure 6: Transmission of SOH slot-waveguide ring resonator resonators with different slot widths fabricated with a 248 nm DUV lithography.

Table 1: Characteristics of the fabricated SOH slot-waveguide ring resonator resonators.

circumference [μm]	slot width [nm]	center wavelength [nm]	FWHM [nm]	FSR [nm]	Q-factor
69.3	130	1598.03	0.31465	6.7	5079
69.3	150	1586.5	0.47424	7	3345
95.5	130	1597.05	0.05497	3.3	29054
95.5	110	1573.58	0,01567	3.4	100420

6 STAGE OF THE RESEARCH

Three year of research will be needed. The first year has been completed successfully. This period included a first concept development and optimization through numerical simulations as well as a first design realization. Figure of merits such as field confinement factors and nonlinear effective areas of slot-waveguide structures are calculated and presented at the EOSAM 2014 in Berlin as an oral presentation (Steglich et al., 2014). Further simulation results and SOI slot-waveguide design trade-offs will be presented at the PHOTOPTICS 2015 in Berlin as FULL paper with an oral presentation (Steglich et al., 2015a) and at the CLEO/Europe 2015 in Munich (Steglich et al., 2015b). Beside theoretical investigations, first electro-optical modulators have been fabricated with a SiGe BiCMOS pilot line at the IHP. We expect to demonstrate our first measurements on SOH modulator during the next few months.

ACKNOWLEDGEMENTS

REFERENCES

Agrawal, G. (2012). *Nonlinear Fiber Optics*. Academic Press, 5 edition.

Almeida, V. R., Xu, Q., Barrios, C. A., and Lipson, M. (2004). Guiding and confining light in void nanostructure. *Opt. Lett.*, 29(11):1209–1211.

Barrios, C. A., Gylfason, K. B., Sánchez, B., Griol, A., Sohlström, H., Holgado, M., and Casquel, R. (2007). Slot-waveguide biochemical sensor. *Opt. Lett.*, 32(21):3080–3082.

Claes, T., Molera, J., De Vos, K., Schachtb, E., Baets, R., and Bienstman, P. (2009). Label-free biosensing with a slot-waveguide-based ring resonator in silicon on insulator. *Photonics Journal, IEEE*, 1(3):197–204.

Dalton, L. R., Sullivan, P. A., and Bale, D. H. (2010). Electric field poled organic electro-optic materials: State of the art and future prospects. *Chemical Reviews*, 110(1):25–55.

Dell'Olio, F. and Passaro, V. M. (2007). Optical sensing by optimized silicon slot waveguides. *Opt. Express*, 15(8):4977–4993.

Feng, N.-N., Michel, J., and Kimerling, L. (2006). Optical field concentration in low-index waveguides. *Quantum Electronics, IEEE Journal of*, 42(9):885–890.

Gould, M., Baehr-Jones, T., Ding, R., Huang, S., Luo, J., Jen, A. K.-Y., Fedeli, J.-M., Fournier, M., and Hochberg, M. (2011). Silicon-polymer hybrid slot waveguide ring-resonator modulator. *Opt. Express*, 19(5):3952–3961.

Koos, C., Jacome, L., Poulton, C., Leuthold, J., and Freude, W. (2007). Nonlinear silicon-on-insulator waveguides for all-optical signal processing. *Opt. Express*, 15(10):5976–5990.

Korn, D., Jazbinsek, M., Palmer, R., Baier, M., Alloatti, L., Yu, H., Bogaerts, W., Lepage, G., Verheyen, P., Absil, P., Guenter, P., Koos, C., Freude, W., and Leuthold, J. (2014). Electro-optic organic crystal silicon high-speed modulator. *Photonics Journal, IEEE*, 6(2):1–9.

Korn, D., Palmer, R., Yu, H., Schindler, P. C., Alloatti, L., Baier, M., Schmogrow, R., Bogaerts, W., Selvaraja, S. K., Lepage, G., Pantouvaki, M., Wouters, J. M., Verheyen, P., Campenhout, J. V., Chen, B., Baets, R., Absil, P., Dinu, R., Koos, C., Freude, W., and Leuthold, J. (2013). Silicon-organic hybrid (soh) iq modulator using the linear electro-optic effect for transmitting 16qam at 112 gbit/s. *Opt. Express*, 21(11):13219–13227.

Leuthold, J., Koos, C., Freude, W., Alloatti, L., Palmer, R., Korn, D., Pfeifle, J., Lauermann, M., Dinu, R., Wehrli,

S., et al. (2013). Silicon-organic hybrid electro-optical devices. *Selected Topics in Quantum Electronics, IEEE Journal of*, 19(6):3401413–3401413.

Liu, Y., Baehr-Jones, T., Li, J., Pomerene, A., and Hochberg, M. (2011). Efficient strip to strip-loaded slot mode converter in silicon-on-insulator. *Photonics Technology Letters, IEEE*, 23(20):1496–1498.

Palik, E. D. (1997). *Handbook of Optical Constants of Solids*. Academic Press, 1 edition.

Palmer, R., Alloatti, L., Korn, D., Heni, W., Schindler, P., Bolten, J., Karl, M., Waldow, M., Wahlbrink, T., Freude, W., Koos, C., and Leuthold, J. (2013a). Low-loss silicon strip-to-slot mode converters. *Photonics Journal, IEEE*, 5(1):2200409–2200409.

Palmer, R., Alloatti, L., Korn, D., Schindler, P., Baier, M., Bolten, J., Wahlbrink, T., Waldow, M., Dinu, R., Freude, W., Koos, C., and Leuthold, J. (2013b). Low power mach-zehnder modulator in silicon-organic hybrid technology. *Photonics Technology Letters, IEEE*, 25(13):1226–1229.

Palmer, R., Alloatti, L., Korn, D., Schindler, P., Schmogrow, R., Heni, W., Koenig, S., Bolten, J., Wahlbrink, T., Waldow, M., Yu, H., Bogaerts, W., Verheyen, P., Lepage, G., Pantouvaki, M., Van Campenhout, J., Absil, P., Dinu, R., Freude, W., Koos, C., and Leuthold, J. (2013c). Silicon-organic hybrid mzi modulator generating ook, bpsk and 8-ask signals for up to 84 gbit/s. *Photonics Journal, IEEE*, 5(2):6600907–6600907.

Palmer, R., Koeber, S., Woessner, M., Elder, D. L., Heni, W., Korn, D., Yu, H., Lauermann, M., Bogaerts, W., Dalton, L. R., Freude, W., Leuthold, J., and Koos, C. (2014). High-speed silicon-organic hybrid (soh) modulators with 230 pm/v electro-optic coefficient using advanced materials. In *Optical Fiber Communication Conference*, page M3G.4. Optical Society of America.

Robinson, J. T., Preston, K., Painter, O., and Lipson, M. (2008). First-principle derivation of gain in high-index-contrast waveguides. *Opt. Express*, 16(21):16659–16669.

Steglich, P., Padilla Michel, Y., Villringer, C., Dümecke, S., Casalboni, M., and Schrader, S. (2014). Numerical simulation of silicon-organic hybrid slot-waveguides. European Optical Society Annual Meeting (EOSAM).

Steglich, P., Padilla Michel, Y., Villringer, C., Dümecke, S., Casalboni, M., and Schrader, S. (2015a). Silicon-on-insulator slot-waveguide design trade-offs. PHOTOPTICS.

Steglich, P., Villringer, C., Dümecke, S., Padilla Michel, Y., Casalboni, M., and Schrader, S. (2015b). Investigation of optical field confinement of silicon-on-insulator slot-waveguides for integrated electro-optical modulator. CLEO.

Tsang, H., Wong, C., Liang, T., Day, I., Roberts, S., Harpin, A., Drake, J., and Asghari, M. (2002). Optical dispersion, two-photon absorption and self-phase modulation in silicon waveguides at 1.5 μm wavelength. *Applied Physics Letters*, 80(3):416–418.

Vivien, L. and Pavesi, L., editors (2013). *Handbook of Silicon Photonics*. CRC Press, 0 edition.

Weimann, C., Schindler, P. C., Palmer, R., Wolf, S., Bekele, D., Korn, D., Pfeifle, J., Koeber, S., Schmogrow, R., Alloatti, L., Elder, D., Yu, H., Bogaerts, W., Dalton, L. R., Freude, W., Leuthold, J., and Koos, C. (2014). Silicon-organic hybrid (soh) frequency comb sources for terabit/s data transmission. *Opt. Express*, 22(3):3629–3637.